

Targeting CD133 in the enhancement of chemosensitivity in oral squamous cell carcinoma–derived side population cancer stem cells

Cheng-Chia Yu, PhD,^{1,2,3} Fang-Wei Hu, DDS, PhD,^{1,2} Chuan-Hang Yu, DDS, PhD,^{1,2} Ming-Yung Chou, DDS, PhD^{1,2,3*}

¹School of Dentistry, Chung Shan Medical University, Taichung, Taiwan, ²Department of Dentistry, Chung Shan Medical University Hospital, Taichung, Taiwan, ³Institute of Oral Sciences, Chung Shan Medical University, Taichung, Taiwan.

Accepted 18 December 2014

Published online 4 June 2015 in Wiley Online Library (wileyonlinelibrary.com). DOI 10.1002/hed.23975

ABSTRACT: *Background.* Oral squamous cell carcinoma (OSCC) is one of the most common cancers in the world. Previously, we enriched a subpopulation of OSCC-derived cancer stem cells (OSCC-CSCs), and identified CD133 as an OSCC-CSC marker.

Method. We determined the function of CD133 on chemosensitivity of oral cancer CSCs by silencing CD133.

Results. Initially, we observed that the expression profile of CD133 in OSCC-side population (OSCC-SPs) cells, which exerted properties of CSCs, was significantly upregulated than that of major population (MPs) cells of OSCCs. The cell viability experiments showed that SPs were more chemoresistant compared with major populations. Importantly, tar-

geting CD133 ameliorated the drug resistance of OSCC-SPs to cisplatin treatment. Targeting CD133 and cisplatin co-treatment led to the maximal inhibition on tumor initiating properties in OSCC-SPs.

Conclusion. Side population cells with CSCs properties existed in OSCCs, and silencing CD133 exhibited a prominent therapeutic effect in enhancing the sensitivity of chemotherapy in OSCC through elimination of CSCs. © 2015 Wiley Periodicals, Inc. *Head Neck* 38: E231–E238, 2016

KEY WORDS: oral squamous cell carcinomas, chemosensitivity, CD133, cancer stem cells, side population

INTRODUCTION

Oral squamous cell carcinoma (OSCC) is a lethal cancer with clinical, pathological, phenotypical, and biological heterogeneity.¹ In spite of improvements in the diagnosis and management of OSCC, long-term survival rates have improved only marginally over the past decade.² The increasing interest in the cancer stem cell (CSC) model is dramatically altering the current directions in cancer treatments and drug developments.³ We identified a subpopulation of oral cancer-derived CSCs from OSCC cells by sphere formation assay.⁴ Oral cancer-CSCs have been known to have the capacity to promote tumor progression and metastasis, and also contribute to chemoresistance.^{5–11} Side population technology by Hoechst dye exclusion property is among the successful methodologies for CSC isolation.¹² However, the molecular mechanisms by which to regulate the biological properties of side population cells from OSCCs have not been well characterized.

CD133, a 5-transmembrane glycoprotein, is a hematopoietic stem cell and endothelial progenitor marker and seems to be involved in angiogenesis.^{13,14} CD133 expression has been suggested to serve as a prognostic signature for tumor regrowth, malignant progression, and tumor stages in leukemia, brain tumors, retinoblastoma, renal tumors, pancreatic tumors, colon carcinoma, prostate carcinoma, hepatocellular carcinoma, thyroid carcinoma, melanoma, and oral cancer.^{6,15–20} CD133 has been shown to negatively correlate with the survival prognosis of patients with OSCC.⁶ However, the role of CD133 in OSCC-CSCs has yet to be explored.

Herein, we demonstrated a critical role of CD133, which was upregulated in side population cells and previously identified OSCC-CSCs,⁶ in the regulation of chemosensitivity of OSCC-CSCs. Overall, downregulation CD133 ameliorated the drug resistance of OSCC-CSCs to cisplatin treatment. Synergistic effects of targeting CD133 and cisplatin chemotherapy treatment attenuated tumor initiating cells property in OSCC-CSCs. Thus, our study implicates that targeting CD133 would be a valuable therapeutic clinically in combination with conventional chemotherapy treatment modalities for malignant OSCC.

MATERIALS AND METHODS

Side population analysis

OSCC cell lines were suspended at 1×10^6 /mL in pre-warmed Dulbecco modified Eagle's medium (DMEM) with 2% fetal bovine serum (FBS). Hoechst 33342 dye was added at a final concentration of 5 μ g/mL in the presence

*Corresponding author: M.-Y. Chou, School of Dentistry, Chung Shan Medical University, No. 110, Sec. 1, Jiaanguo N. Road, Taichung 40201, Taiwan. E-mail: myc@csmu.edu.tw

This article was published online 4 June 2015. This notice indicates Figure 2c has been corrected.

Contract grant sponsor: This study was supported by a research grant from Chung Shan Medical University Hospital (GSH-2014-D-001) and the Ministry of Science and Technology (MOST 103-2632-B-040-001) in Taiwan, Republic of China

or absence of verapamil (50 μ M; Sigma, St Louis, MO) and was incubated at 37°C for 90 minutes with intermittent shaking. Then the cells were washed with ice-cold Hanks buffered salt solution with 2% FBS and centrifuged at 4°C, and resuspended in ice-cold Hanks buffered salt solution containing 2% FBS. Propidium iodide at a final concentration of 2 μ g/mL was added to the cells to gate viable cells. The Hoechst 33342 dye was excited at 357 nm and its fluorescence was dual-wavelength analyzed (blue, 402–446 nm; red, 650–670 nm). Analyses were done on a FACS Vantage (BD Biosciences, San Diego, CA).

Tumor spheres assay

Spheres from OSCC cells were isolated in medium consisting of serum-free DMEM/F12 medium (Gibco, Grand Island, NY), N2 supplement (Gibco), 10 ng/mL human recombinant basic fibroblast growth factor, and 10 ng/mL epidermal growth factor (R&D Systems, Minneapolis, MN). Cells were plated at a density of 10⁴ live cells/10-mm low attachment dishes, and the medium was changed every other day until the tumor sphere formation was observed in about 1 week.²¹

In vitro cell invasion assay

Invasion assays were done in 24-well Transwell units with an 8.0 μ m porous transparent polyethylene terephthalate

membrane. Cells (1 \times 10⁵ per well) were added to upper chambers (filter coated with 1 mg/mL Matrigel) in 100 μ L of the low serum medium. The lower chambers were filled with 500 μ L high serum medium. After 24 hours of incubation at 37°C, cells that remained in the Matrigel or attached to the upper side of the filter were removed with cotton swabs. Cells that had migrated through the membrane to the lower surface were stained with Hoechst 33258 and counted in 5 different fields under a fluorescence microscope.²²

Soft agar colony forming assay

Each well (35 mm) of a 6-well culture dish was coated with 2 mL bottom agar (Sigma–Aldrich) mixture (DMEM, 10% [v/v] fetal calf serum, 0.6% [w/v] agar). After the bottom layer was solidified, 2 mL top agar-medium mixture (DMEM, 10% [v/v] fetal calf serum, 0.3% [w/v] agar) containing 2 \times 10⁴ cells was added, and the dishes were incubated at 37°C for 4 weeks. Plates were stained with 0.005% Crystal Violet then the colonies were counted. The number of total colonies with a diameter \geq 100 μ m was counted over 5 fields per well for a total of 15 fields in triplicate experiments.

Subcutaneous xenografts in nude mice

The animal study was approved by the Institutional Animal Care and Use Committee in Chung Shan

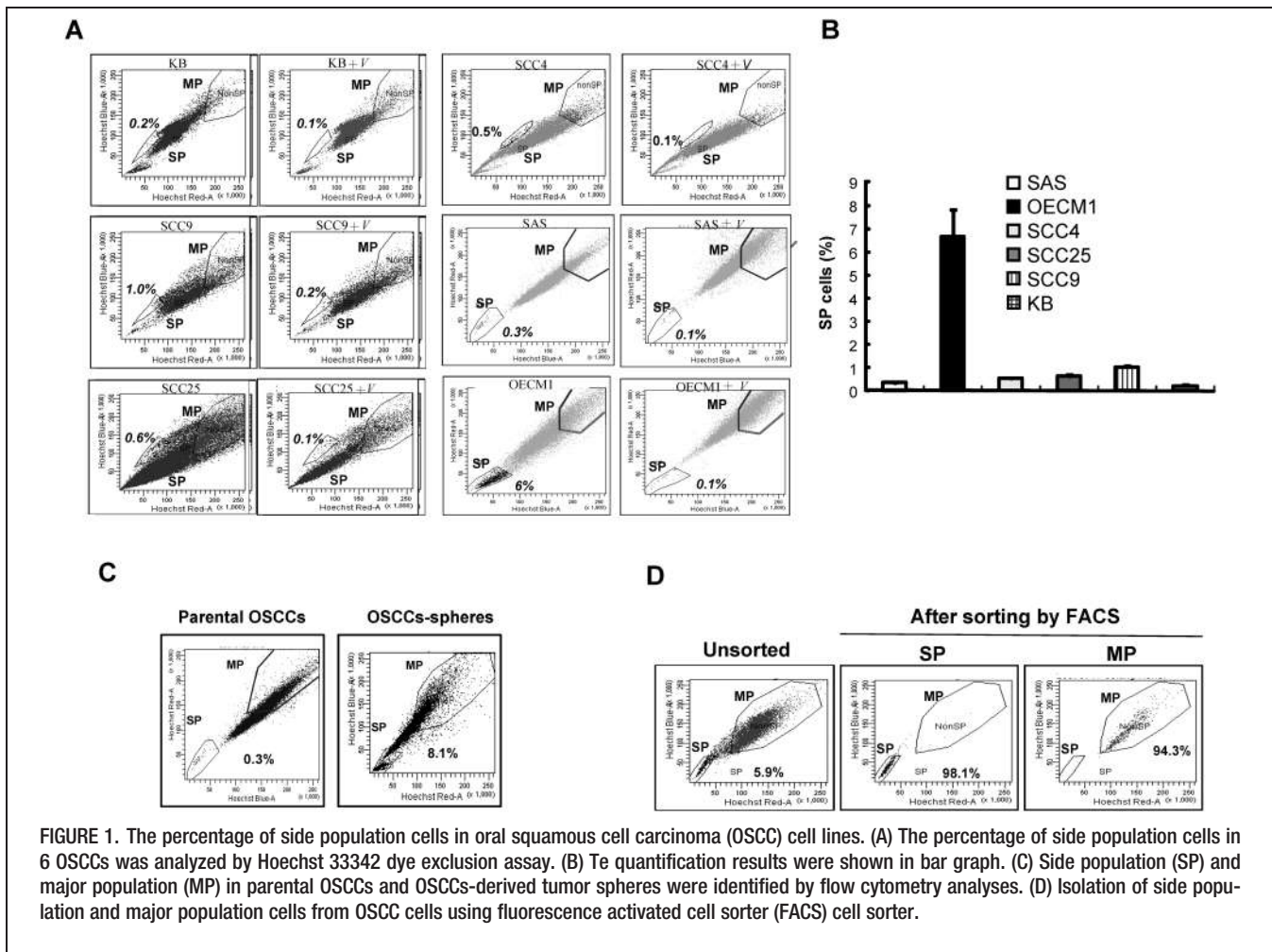


FIGURE 1. The percentage of side population cells in oral squamous cell carcinoma (OSCC) cell lines. (A) The percentage of side population cells in 6 OSCCs was analyzed by Hoechst 33342 dye exclusion assay. (B) The quantification results were shown in bar graph. (C) Side population (SP) and major population (MP) in parental OSCCs and OSCCs-derived tumor spheres were identified by flow cytometry analyses. (D) Isolation of side population and major population cells from OSCC cells using fluorescence activated cell sorter (FACS) cell sorter.

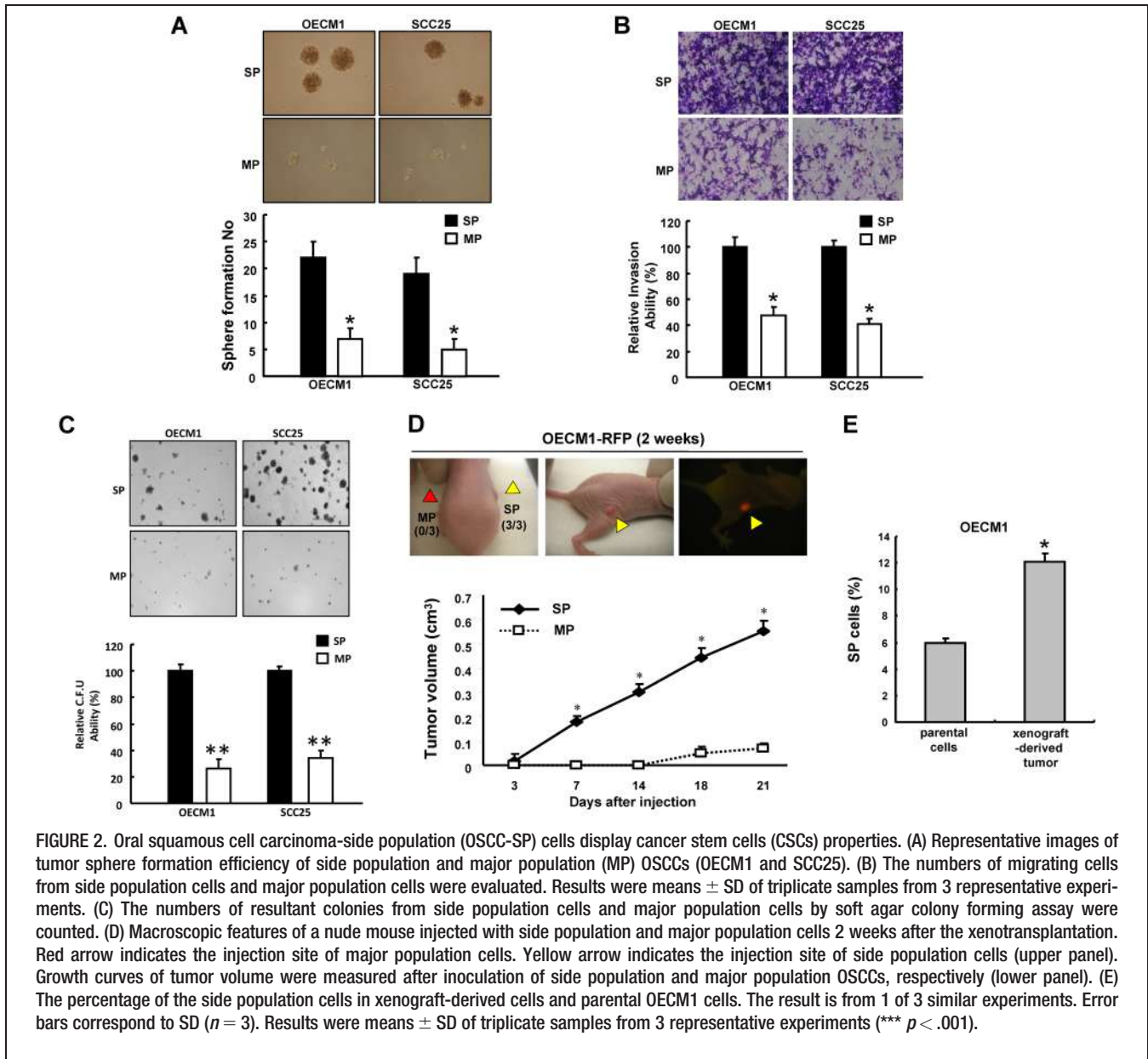


FIGURE 2. Oral squamous cell carcinoma-side population (OSCC-SP) cells display cancer stem cells (CSCs) properties. (A) Representative images of tumor sphere formation efficiency of side population and major population (MP) OSCCs (OECM1 and SCC25). (B) The numbers of migrating cells from side population cells and major population cells were evaluated. Results were means \pm SD of triplicate samples from 3 representative experiments. (C) The numbers of resultant colonies from side population cells and major population cells by soft agar colony forming assay were counted. (D) Macroscopic features of a nude mouse injected with side population and major population cells 2 weeks after the xenotransplantation. Red arrow indicates the injection site of major population cells. Yellow arrow indicates the injection site of side population cells (upper panel). Growth curves of tumor volume were measured after inoculation of side population and major population OSCCs, respectively (lower panel). (E) The percentage of the side population cells in xenograft-derived cells and parental OECM1 cells. The result is from 1 of 3 similar experiments. Error bars correspond to SD ($n = 3$). Results were means \pm SD of triplicate samples from 3 representative experiments (***) $p < .001$.

Medical University (permit number: 935). All procedures were performed with the mice under anesthesia, and efforts were made to minimize animal suffering during experiments by following the guidelines. OSCC cells mixed with Matrigel (1:1; BD Bioscience) were injected subcutaneously into BALB/c nude mice (6–8 weeks). Tumor volume was calculated using the following formula: tumor volume (mm^3) = (length \times width²)/2.

Flow cytometry for cell surface marker analysis

Cells were stained with anti-CD133 antibody (Miltenyi Biotech, Auburn, CA) and anti-ABCG2 antibody (Chemicon, Temecula, CA) with labeling according to the manufacturer's instructions. Fluorescence emission from 10,000

cells was measured with an FACS Calibur (Becton Dickinson, San Jose, CA) using CellQuest software.

ALDEFLUOR assay

An ALDEFLUOR assay kit was purchased from StemCell Technologies, Inc. (Vancouver, British Columbia, Canada). For this assay, 1×10^5 cells were suspended in 50 μL of assay buffer, and ALDEFLUOR was added to the cell suspensions for a final concentration of 1 μM . For aldehyde dehydrogenase 1 (ALDH1) inhibitor control, diethylamino-benzaldehyde was added to a final concentration of 150 μM . Cells were then incubated at 37°C for 45 minutes and were stained with 7-amino-actinomycin D on ice for 5 minutes. After washing the cells with phosphate-buffered saline, live cells (7-amino-actinomycin D)-positive for green fluorescence were analyzed by flow cytometry to compare the

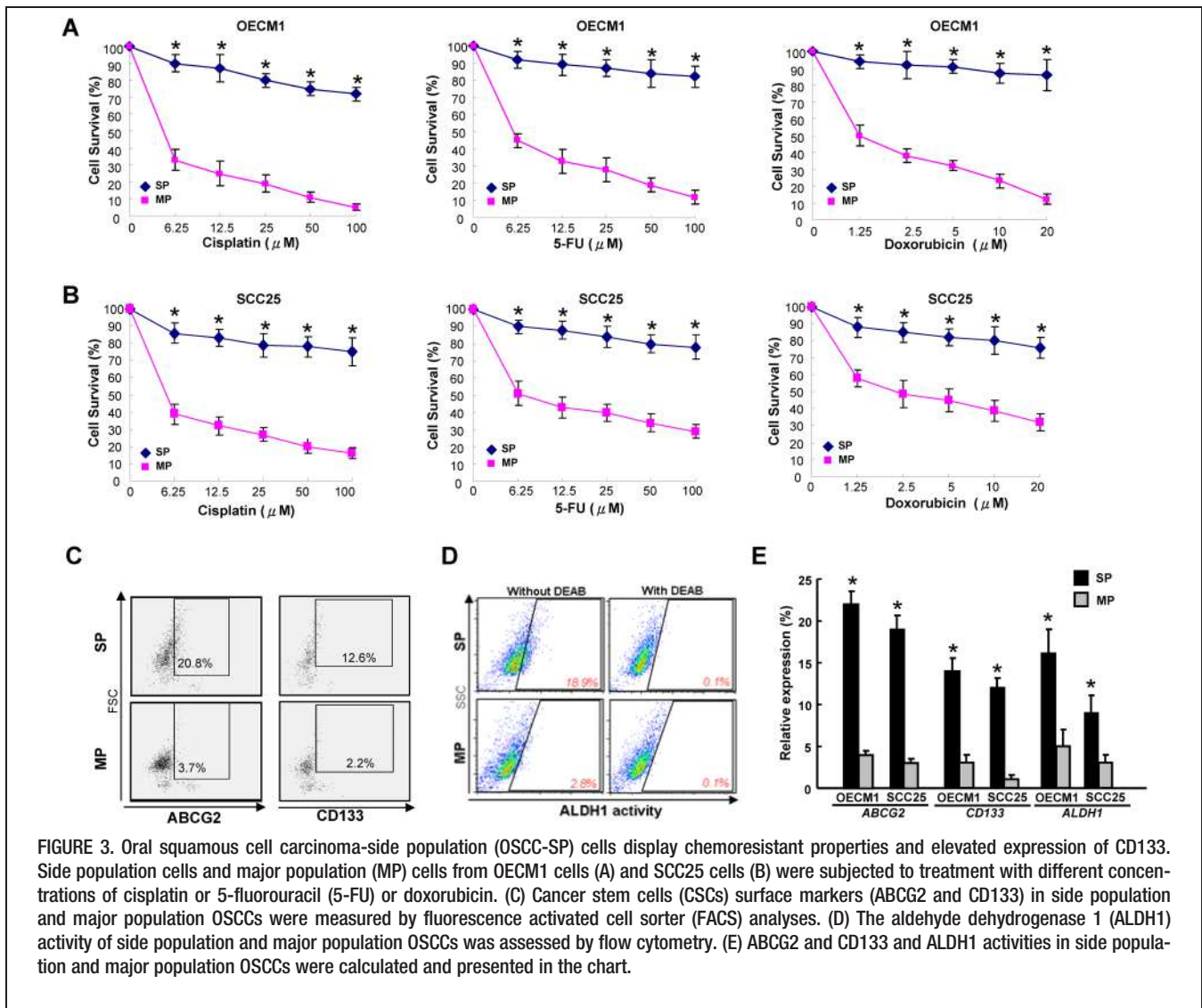


FIGURE 3. Oral squamous cell carcinoma-side population (OSCC-SP) cells display chemoresistant properties and elevated expression of CD133. Side population cells and major population (MP) cells from OECC1 cells (A) and SCC25 cells (B) were subjected to treatment with different concentrations of cisplatin or 5-fluorouracil (5-FU) or doxorubicin. (C) Cancer stem cells (CSCs) surface markers (ABCG2 and CD133) in side population and major population OSCCs were measured by fluorescence activated cell sorter (FACS) analyses. (D) The aldehyde dehydrogenase 1 (ALDH1) activity of side population and major population OSCCs was assessed by flow cytometry. (E) ABCG2 and CD133 and ALDH1 activities in side population and major population OSCCs were calculated and presented in the chart.

fluorescence intensity of the diethylaminobenzaldehyde-treated samples. High fluorescence was associated with high ALDH activity (ALDH+ cells).

Stable silencing of CD133 by lentiviral vector

The pLV-RNAi vector was purchased from Biosettia (Biosettia, San Diego, CA). The method of cloning the double-stranded short hairpin RNA (shRNA) sequence is described in the manufacturer's protocol. Lentiviral vectors expressing shRNA that targets human CD133 (oligonucleotide sequence: *Sh-CD133-1*:5'-AAAAGGACAAGGCGTTCACAGATT TGGATCCAAATCTGTGAACGCCT TGTCC-3'; *Sh-CD133-2*:5'-AAAAGGATACACCCT ACT TACTATTGGATCCAATAGTAAGTAGGGTGTATCC-3') were synthesized and cloned into pLVRNAi to generate a lentiviral expression vector. Lentivirus production was performed by transfection of plasmid DNA mixture with lentivector plus helper plasmids (VSVG and Gag-Pol) into 293T cells using lipofectamine 2000 (LF2000; Invitrogen, Cals-

bad, CA). The green fluorescent protein positive cells were cells expressing the shRNA for silencing CD133.

Cell proliferation assay

Methyl thiazolyl-tetrazolium (MTT) assay kit (Sigma-Aldrich, Oakville, Ontario, Canada) was used to analyze the cell proliferation. Specifically, 1×10^3 cells were seeded in each well of a 24-well plate, and then 10 μ L of MTT solution was added to the cells, which were then incubated at 37°C for 3 hours. The supernatant was removed, and 200 μ L of dimethyl sulfoxide were added directly to the cells. The MTT color reaction was analyzed using a microplate reader set at A560 nm.

Statistical analysis

Statistical Package of Social Sciences software version 13.0 (SPSS, Chicago, IL) was used for statistical analysis. Student's *t* test was used to determine statistical significance of the differences between experimental groups; *p* values < .05 were considered statistically

significant. The level of statistical significance was set at .05 for all tests.

RESULTS

Existence of side population cells in oral squamous cell carcinoma cells

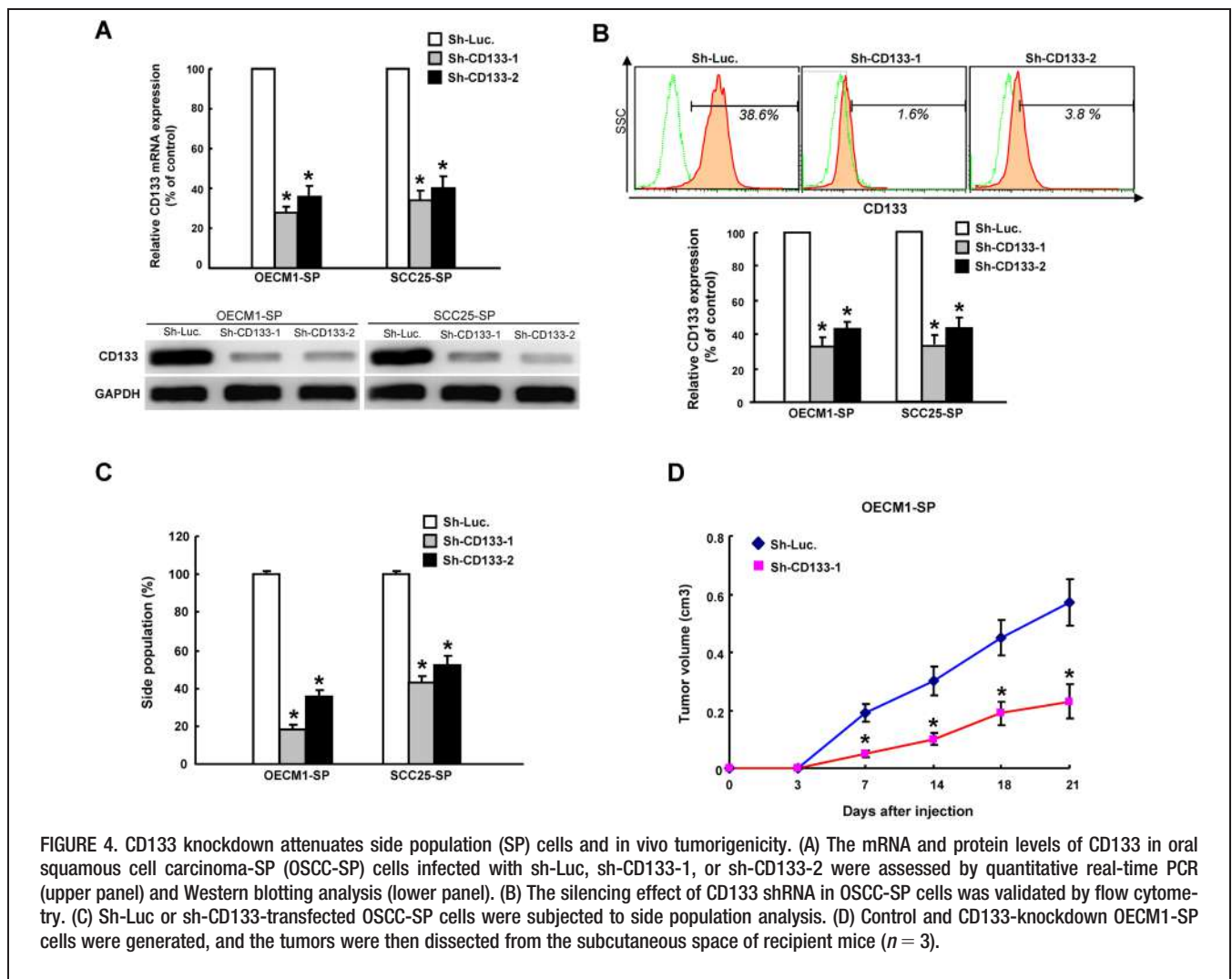
Side population cells have been found to have characteristics of CSCs.²³ We also found that about 0.1% to 6.0% of side population cells existed in 6 OSCCs (Figure 1A and 1B). Previously, we and others have isolated OSCC-CSCs through tumor spheres assay.^{6,24} To elucidate the relationship between side population cells and sphere-forming CSCs, the amount of side population cells in OSCCs-derived tumor spheres was first examined. Apparently, OSCCs-derived tumor spheres contained more side population cells than the parental OSCCs (Figure 1C). To further understand whether side populations have the tumor initiating characteristics, OECM1 and SCC25 cells were sorted into side population cells and major population cells by flow cytometry (Figure 1D).

OSCC-derived side population (OSCC-SP) cells display tumorigenic potentials cancer initiating cells properties and elevated expression of CD133.

We next performed tumor sphere assays to evaluate the self-renewal ability of OSCC-SP and OSCC-derived MP (OSCC-MP) cells, respectively. Interestingly, OSCC-SP cells from OECM1 cells displayed higher tumor sphere-forming capability than OSCC-MP cells did (Figure 2A). Next, the in vitro and in vivo tumorigenic activities between OSCC-SP and OSCC-MP cells were compared. The invasiveness/colony formation abilities of OSCC-SP cells were also significantly higher than those of the OSCC-MP cells (Figure 2B and 2C). Furthermore, injection of 10⁴ OSCC-MP cells into nude mice did not lead to tumor formation, but nude mice administrated with 10⁴ OSCC-SP cells displayed visible tumors 3 weeks after injection (Figure 2D). Interestingly, the xenograft-derived cells were enriched for side population cells more than the parental cell line (Figure 2E).

Oral squamous cell carcinoma-side population cells elevated chemoresistance and expression of CD133

Because resistance to chemotherapy treatment is a major clinical criterion for characterizing CSCs in OSCC, we then evaluated the chemosensitivity of side population and major population cells, respectively. Cell viability assays showed that side population cells were more



chemoresistant to cisplatin, 5-fluorouracil or doxorubicin treatment compared with the major population cells of both OECM1 (Figure 3A) and SCC25 (Figure 3B) cells. Finally, the side population cells expressed higher a level of the drug resistance-related gene and specific surface markers (ABCG2 and CD133; Figure 3C and 3E). A similar upregulation of CSCs marker ALDH1 activity was also observed in side population cells when compared with major population cells (Figure 3D and 3E). Together, we hypothesized that upregulation of CD133 might be crucial for modulating chemosensitivity of OSCC-CSCs.

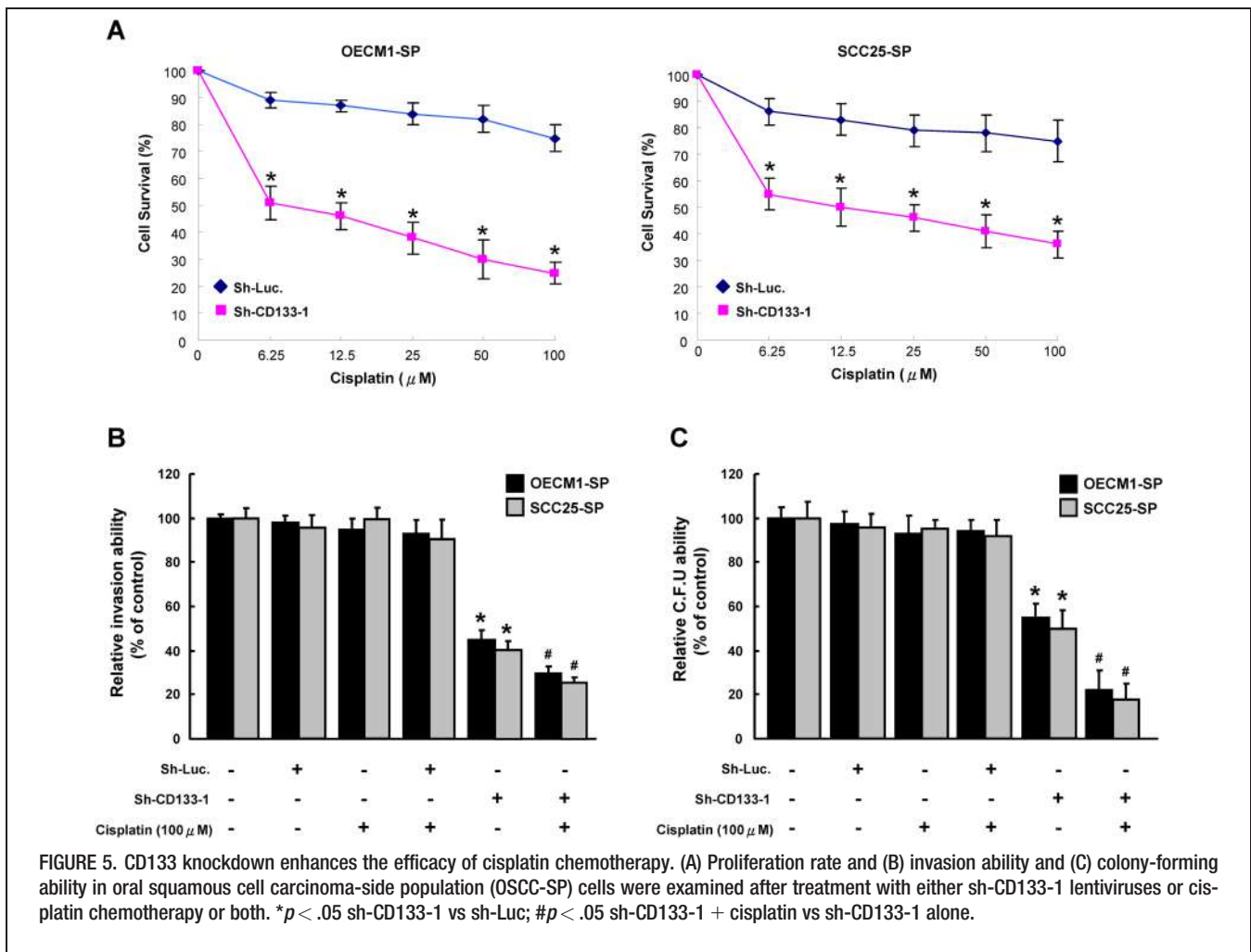
Diminished side population and in vivo tumorigenicity in oral squamous cell carcinoma-side population by targeting CD133

To further investigate the functional role of CD133 on oncogenicity, subsequently, approach of loss-of-function of CD133 through lentiviral-mediated transduction was conducted in OSCC-SP. Real-time reverse transcriptase-polymerase chain reaction and immunoblotting analyses confirmed that lentivirus expressing both sh-CD133-1 and sh-CD133-2 markedly reduced the expression level of CD133 mRNA (Figure 4A, upper panel) and protein (Fig-

ure 4A, lower panel) in transduced OSCC-SP. Flow cytometry analyses confirmed that both sh-CD133-1 and sh-CD133-2 markedly reduced the expression of CD133 protein in OSCC-SP (Figure 4B). Silencing CD133 decreased the percentage of side population cells in both OECM1 and SCC25 cells (Figure 4C). Furthermore, inhibition of CD133 expression significantly attenuated the in vivo tumor growth of nude mice mediated by OSCC-SP cells (Figure 4D).

Downregulation of CD133 enhanced chemosensitivity in oral squamous cell carcinoma-side population

The combination CD133-knockdown and cisplatin treatment showed a synergistic effect in abrogating proliferation rate in OSCC-SP (Figure 5A). Single cell suspension of CD133-knockdown OSCC-SP treated with or without cisplatin treatment was used for analysis of their invasion/clonogenicity in vitro as described in the Materials and Methods section. Treatment with cisplatin alone did not affect the invasion ability in OSCC-SP cells (Figure 5B), the combination of silencing CD133 and cisplatin treatment enhanced the efficacy of these treatments (Figure 5B). Meanwhile, similar synergistic effect of downregulation of CD133 and chemotherapy treatment was



also observed in colony formation assay (Figure 5C). Taken together, targeting CD133 exhibited a prominent therapeutic effect in enhancing the sensitivity of chemotherapy in OSCC-CSCs.

DISCUSSION

During the last decades, the existence and the identity of CSCs have been identified in hematopoietic tumors as well as a variety range of solid tumors, including breast, brain, lung, colon, prostate, head and neck, and others.^{5,18,25–32} Breast cancer was the first solid tumor in which CSCs was isolated: the breast CSCs was characterized as a minority population (<5%) of cells expressing high levels of CD44 and low levels of CD24 cell surface markers.³³ Colon, lung, and hematopoietic CSCs are isolated by cell sorting with the expression of CD133,^{29,30,34–36} although the function of CD133 is still unclear. These cells grow indefinitely as spheres in vitro and were tumorigenic in vivo.³⁰ Hoechst 33342 staining CSCs are enriched in the side populations of cancer cells, excluding intracellular Hoechst 33342 in vitro,^{37,38} and can be isolated by flow cytometry. Expression of ABCG2, an ATPase transporter, in CSCs is found closely associated with its specific exclusion capacity, rendering ABCG2 a CSCs marker in some cases.³⁹ Similar with our studies, OSCC-SP cells present with elevated cancer stemness markers (Oct4, ABCG2, and EpCAM) and are highly tumorigenic and resistant to chemotherapy.⁴⁰ In the present study, we demonstrated that side population cells of OSCCs exerted CSCs properties, and expression of CD133 was significantly upregulated in side population cells (Figures 1 and 3). Consequently, we evaluated the role of CD133 in the chemosensitivity and tumorigenic potential of oral cancer CSCs by lentiviral-mediated knockdown of CD133 (Figures 4 and 5). We showed in OSCC-SP cells that depletion of CD133 led to a high tolerance of OSCC-SP cells to cisplatin or fluorouracil treatment.

The miRNAs seem to function as either oncogenes or tumor suppressors, cell cycle regulators, and transcription factors, and are involved in many aspects of OSCC.^{41,42} Accumulating evidence has been reported supporting the involvement of miRNAs in CSCs properties.^{43–46} For example, miR34 overexpression impairs the self-renewal properties of brain tumor and pancreatic cancer stem cells.⁴⁵ The miR200b regulates CSCs properties through directly targeting Suz12, a subunit of a polycomb repressor complex.⁴⁷ Ectopic let-7a,¹⁰ miR200c,⁸ and miR145⁴⁸ expression suppress the tumorigenicity of OSCC-CSCs. Recently, miR-142-3p reduced the self-renewal, tumor regeneration, chemo-resistance, and metastasis properties in hepatocellular carcinoma through directly targeting CD133.⁴⁹ It is therefore possible that CD133 might also be regulated by miRNAs in OSCC-CSCs. Further research effort is needed in this area.

CONCLUSION

Overall, our present research showed OSCCs-derived side population cells displayed CSCs characteristics and targeting CD133 sensitized CSCs to chemotherapies. Our results provide insights into the clinical prospect of CD133-based therapies for OSCC.

REFERENCES

- Haddad RI, Shin DM. Recent advances in head and neck cancer. *N Engl J Med* 2008;359:1143–1154.
- Jemal A, Siegel R, Ward E, et al. Cancer statistics, 2008. *CA Cancer J Clin* 2008;58:71–96.
- Visvader JE, Lindeman GJ. Cancer stem cells in solid tumours: accumulating evidence and unresolved questions. *Nat Rev Cancer* 2008;8:755–768.
- Chang WW, Hu FW, Yu CC, et al. Quercetin in elimination of tumor initiating stem-like and mesenchymal transformation property in head and neck cancer. *Head Neck* 2013;35:413–419.
- Prince ME, Sivanandan R, Kaczorowski A, et al. Identification of a subpopulation of cells with cancer stem cell properties in head and neck squamous cell carcinoma. *Proc Natl Acad Sci U S A* 2007;104:973–978.
- Chiou SH, Yu CC, Huang CY, et al. Positive correlations of Oct-4 and Nanog in oral cancer stem-like cells and high-grade oral squamous cell carcinoma. *Clin Cancer Res* 2008;14:4085–4095.
- Wu MJ, Jan CI, Tsay YG, et al. Elimination of head and neck cancer initiating cells through targeting glucose regulated protein78 signaling. *Mol Cancer* 2010;9:283.
- Lo WL, Yu CC, Chiou GY, et al. MicroRNA-200c attenuates tumour growth and metastasis of presumptive head and neck squamous cell carcinoma stem cells. *J Pathol* 2011;223:482–495.
- Lo JF, Yu CC, Chiou SH, et al. The epithelial-mesenchymal transition mediator S100A4 maintains cancer-initiating cells in head and neck cancers. *Cancer Res* 2011;71:1912–1923.
- Yu CC, Chen YW, Chiou GY, et al. MicroRNA let-7a represses chemoresistance and tumorigenicity in head and neck cancer via stem-like properties ablation. *Oral Oncol* 2011;47:202–210.
- Chen YS, Wu MJ, Huang CY, et al. CD133/Src axis mediates tumor initiating property and epithelial-mesenchymal transition of head and neck cancer. *PLoS One* 2011;6:e28053.
- Hadnagy A, Gaboury L, Beaulieu R, Balicki D. SP analysis may be used to identify cancer stem cell populations. *Exp Cell Res* 2006;312:3701–3710.
- Corbeil D, Röper K, Hellwig A, et al. The human AC133 hematopoietic stem cell antigen is also expressed in epithelial cells and targeted to plasma membrane protrusions. *J Biol Chem* 2000;275:5512–5520.
- Hilbe W, Dirnhofer S, Oberwasserlechner F, et al. CD133 positive endothelial progenitor cells contribute to the tumour vasculature in non-small cell lung cancer. *J Clin Pathol* 2004;57:965–969.
- Hemmati HD, Nakano I, Lazareff JA, et al. Cancerous stem cells can arise from pediatric brain tumors. *Proc Natl Acad Sci U S A* 2003;100:15178–15183.
- Yin S, Li J, Hu C, et al. CD133 positive hepatocellular carcinoma cells possess high capacity for tumorigenicity. *Int J Cancer* 2007;120:1444–1450.
- Chu P, Clanton DJ, Snipas TS, et al. Characterization of a subpopulation of colon cancer cells with stem cell-like properties. *Int J Cancer* 2009;124:1312–1321.
- Singh SK, Hawkins C, Clarke ID, et al. Identification of human brain tumour initiating cells. *Nature* 2004;432:396–401.
- Vander Griend DJ, Karthaus WL, Dalrymple S, Meeker A, DeMarzo AM, Isaacs JT. The role of CD133 in normal human prostate stem cells and malignant cancer-initiating cells. *Cancer Res* 2008;68:9703–9711.
- Rappa G, Fodstad O, Lorico A. The stem cell-associated antigen CD133 (Prominin-1) is a molecular therapeutic target for metastatic melanoma. *Stem Cells* 2008;26:3008–3017.
- Hu FW, Tsai LL, Yu CH, Chen PN, Chou MY, Yu CC. Impairment of tumor-initiating stem-like property and reversal of epithelial-mesenchymal transdifferentiation in head and neck cancer by resveratrol treatment. *Mol Nutr Food Res* 2012;56:1247–1258.
- Yu CH, Yu CC. Photodynamic therapy with 5-aminolevulinic acid (ALA) impairs tumor initiating and chemo-resistance property in head and neck cancer-derived cancer stem cells. *PLoS One* 2014;9:e87129.
- Chiba T, Kita K, Zheng YW, et al. Side population purified from hepatocellular carcinoma cells harbors cancer stem cell-like properties. *Hepatology* 2006;44:240–251.
- Okamoto A, Chikamatsu K, Sakakura K, Hatsushika K, Takahashi G, Masuyama K. Expansion and characterization of cancer stem-like cells in squamous cell carcinoma of the head and neck. *Oral Oncol* 2009;45:633–639.
- Jiang F, Qiu Q, Khanna A, et al. Aldehyde dehydrogenase 1 is a tumor stem cell-associated marker in lung cancer. *Mol Cancer Res* 2009;7:330–338.
- Lee TK, Castilho A, Cheung VC, Tang KH, Ma S, Ng IO. CD24(+) liver tumor-initiating cells drive self-renewal and tumor initiation through STAT3-mediated NANOG regulation. *Cell Stem Cell* 2011;9:50–63.
- Ibrahim EE, Babaei-Jadidi R, Saadeddin A, et al. Embryonic NANOG activity defines colorectal cancer stem cells and modulates through API-1 and TCF-dependent mechanisms. *Stem Cells* 2012;30:2076–2087.
- Bao S, Wu Q, McLendon RE, et al. Glioma stem cells promote radioresistance by preferential activation of the DNA damage response. *Nature* 2006;444:756–760.
- Bertolini G, Roz L, Perego P, et al. Highly tumorigenic lung cancer CD133+ cells display stem-like features and are spared by cisplatin treatment. *Proc Natl Acad Sci U S A* 2009;106:16281–16286.

30. Eramo A, Lotti F, Sette G, et al. Identification and expansion of the tumorigenic lung cancer stem cell population. *Cell Death Differ* 2008;15:504–514.
31. Bussolati B, Bruno S, Grange C, Ferrando U, Camussi G. Identification of a tumor-initiating stem cell population in human renal carcinomas. *FASEB J* 2008;22:3696–3705.
32. Clay MR, Tabor M, Owen JH, et al. Single-marker identification of head and neck squamous cell carcinoma cancer stem cells with aldehyde dehydrogenase. *Head Neck* 2010;32:1195–1201.
33. Al-Hajj M, Wicha MS, Benito-Hernandez A, Morrison SJ, Clarke MF. Prospective identification of tumorigenic breast cancer cells. *Proc Natl Acad Sci U S A* 2003;100:3983–3988.
34. Yin AH, Miraglia S, Zanjani ED, et al. AC133, a novel marker for human hematopoietic stem and progenitor cells. *Blood* 1997;90:5002–5012.
35. Saigusa S, Tanaka K, Toiyama Y, et al. Correlation of CD133, OCT4, and SOX2 in rectal cancer and their association with distant recurrence after chemoradiotherapy. *Ann Surg Oncol* 2009;16:3488–3498.
36. Wakamatsu Y, Sakamoto N, Oo HZ, et al. Expression of cancer stem cell markers ALDH1, CD44 and CD133 in primary tumor and lymph node metastasis of gastric cancer. *Pathol Int* 2012;62:112–119.
37. Das B, Tsuchida R, Malkin D, Koren G, Baruchel S, Yeger H. Hypoxia enhances tumor stemness by increasing the invasive and tumorigenic side population fraction. *Stem Cells* 2008;26:1818–1830.
38. Ho MM, Ng AV, Lam S, Hung JY. Side population in human lung cancer cell lines and tumors is enriched with stem-like cancer cells. *Cancer Res* 2007;67:4827–4833.
39. Jiang Y, He Y, Li H, et al. Expressions of putative cancer stem cell markers ABCB1, ABCG2, and CD133 are correlated with the degree of differentiation of gastric cancer. *Gastric Cancer* 2012;15:440–450.
40. Yanamoto S, Kawasaki G, Yamada S, et al. Isolation and characterization of cancer stem-like side population cells in human oral cancer cells. *Oral Oncol* 2011;47:855–860.
41. Liu CJ, Shen WG, Peng SY, et al. miR-134 induces oncogenicity and metastasis in head and neck carcinoma through targeting WWOX gene. *Int J Cancer* 2014;134:811–821.
42. Tu HF, Lin SC, Chang KW. MicroRNA aberrances in head and neck cancer: pathogenetic and clinical significance. *Curr Opin Otolaryngol Head Neck Surg* 2013;21:104–111.
43. Garzia L, Andolfo I, Cusanelli E, et al. MicroRNA-199b-5p impairs cancer stem cells through negative regulation of HES1 in medulloblastoma. *PLoS One* 2009;4:e4998.
44. Ji J, Yamashita T, Budhu A, et al. Identification of microRNA-181 by genome-wide screening as a critical player in EpCAM-positive hepatic cancer stem cells. *Hepatology* 2009;50:472–480.
45. Ji Q, Hao X, Zhang M, et al. MicroRNA miR-34 inhibits human pancreatic cancer tumor-initiating cells. *PLoS One* 2009;4:e6816.
46. Silber J, Lim DA, Petritsch C, et al. miR-124 and miR-137 inhibit proliferation of glioblastoma multiforme cells and induce differentiation of brain tumor stem cells. *BMC Med* 2008;6:14.
47. Iliopoulos D, Lindahl-Allen M, Polytarchou C, Hirsch HA, Tsichlis PN, Struhl K. Loss of miR-200 inhibition of Suz12 leads to polycomb-mediated repression required for the formation and maintenance of cancer stem cells. *Mol Cell* 2010;39:761–772.
48. Yu CC, Tsai LL, Wang ML, et al. miR145 targets the SOX9/ADAM17 axis to inhibit tumor-initiating cells and IL-6-mediated paracrine effects in head and neck cancer. *Cancer Res* 2013;73:3425–3440.
49. Chai S, Tong M, Ng KY, et al. Regulatory role of miR-142-3p on the functional hepatic cancer stem cell marker CD133. *Oncotarget* 2014;5:5725–5735.